Research on Engineering Structures & Materials
www.jresm.org
MIM Research Group

Research Article

Paraffin candle soot as a promising hydrophobic coating for gas diffusion layers in PEM fuel cells: An analytical feasibility study

Chijindu Ikechukwu Igwe [*,a]

Department of Mechatronic Systems Engineering, Simon Fraser University, Canada

Article Info

Article History:

Received 14 July 2026

Accepted 12 Oct 2026

Keywords:

Carbon fiber;
Gas diffusion layer;
Hydrophobicity;
Paraffin candle soot;
PTFE

Abstract

Hydrophobicity of the gas diffusion layer (GDL) is critical for efficient water management in polymer electrolyte membrane fuel cells (PEMFCs). Although polytetrafluoroethylene (PTFE) coatings impart hydrophobicity to carbon fiber GDLs, increasing PTFE content reduces through-plane electronic conductivity, while lower PTFE loading promotes liquid water flooding at high current densities. This study proposes paraffin candle soot as an alternative hydrophobic coating for carbon fiber GDLs and evaluates its suitability through interfacial analyses at the gas-liquid-solid interface. Performance metrics included spreading coefficient, contact angle, contact angle hysteresis, and electronic conductivity. The analyses showed that paraffin candle soot exhibits spreading coefficients and water contact angles comparable to PTFE in air, while providing lower contact angle hysteresis, higher electronic conductivity, and good adhesion to carbon fibers. Additionally, the coating remained thermally stable up to 300°C, mechanically stable under pressures up to 5 bar, and chemically stable over a pH range of 1-13. Experimental validation is recommended to confirm these analytical findings. Based on Butler-Volmer kinetics, improved mitigation of liquid water flooding is expected to enhance reactant gas concentration, reduce activation overpotential, increase exchange current density, and accelerate PEMFC electrochemical reaction kinetics. This work is presented as an analytical feasibility assessment, based on established interfacial and electrochemical models populated with literature-derived parameters, and is intended to guide subsequent experimental validation.

© 2026 MIM Research Group. All rights reserved.

1. Introduction

Polymer electrolyte membrane fuel cells (PEMFCs) are galvanic electrochemical devices that facilitate the reaction of hydrogen gas (fuel) and air/oxygen (oxidant) to produce electricity, with water vapor and heat as byproducts [1,2]. Several layers of components make up a PEMFC, including platinum catalyst coated carbon electrodes, polymer membrane, gas diffusion layer, gaskets, and graphite endplates [3,4]. Electrical energy from a PEMFC is considered clean and sustainable if the hydrogen fuel is green [5].

A major component of the PEMFC which facilitates hydrogen and air/oxygen gas transport, and product water management, as well as electrical conductivity – acting as a bridge between the catalyst layer and cell plate is the gas diffusion layer (GDL) [6]. The GDL is desired to be electronically conductive since it is expected to transfer electrons between the catalyst layer and the bipolar plates [7]. Hence, available in the form of carbon paper or woven carbon fabrics [6]. Furthermore, to effectively transport reactant gases, and manage product water, the pores of the GDL are not to be choked with product water [8]. The carbon paper/fabric is, therefore, pre-coated with polytetrafluoroethylene (PTFE), which changes the GDL surface from hydrophilic to

*Corresponding author: chijindu_igwe@sfu.ca
[a]orcid.org/0000-0001-8379-2215
DOI: http://dx.doi.org/10.17515/resm2026-1866ma0714rs

hydrophobic. The design of the GDL is such that it does not get wetted by water. The material surface is optimized for optimal water-residence. This means that the hydrophobic surface of the GDL drains product water from the cell [8], so that the catalyst layer will not be flooded, and the membrane remains hydrated, thus improving the overall catalytic reaction [6]. Properties of the GDL such as permeability, porosity, tortuosity, and hydrophobicity are designed for optimized effective gas diffusivity [8].

Table 1. Interfacial challenges associated with the GDLs in PEMFCs

S/N	Interfacial challenges	References
1	Liquid water flooding	[9]
2	Reactant gas starvation	[10]
3	Hydrophobicity degradation	[11]
4	Carbon corrosion/oxidation & degradation	[12–14]
5	Electrical contact resistance with bipolar plates	[15]
6	Interfacial delamination (swelling & non-uniform compression)	[16]
7	Resistive film formation from undesirable chemical reactions	[17]
8	Ionic contamination from impurities & debris	[18]
9	Surface fouling from undesirable electrochemical byproducts	[19]

In Table 1, a list of interfacial challenges associated with the GDLs in PEMFCs is presented. PTFE treatment and coating of GDL has been used to address liquid water flooding in PEMFCs. PTFE loading between 5 and 30 wt.% [20], optimally 30-35% [6] can be applied to the GDL in several ways. GDL can be dipped into an aqueous PTFE suspension, oven dried, and heated above 350°C. To coat one side of the GDL, techniques such as spraying and brushing are well suited [20]. Unfortunately, treatment and coating with PTFE is found to reduce GDL's electric [7] and thermal conductivity [8], as well as the effective diffusivity [21,22]. Thus, excessive coating with PTFE is detrimental to performance, and improved application methods are highly desired. Through-plane conductivity of GDL with bipolar plates has been investigated and addressed with varying compression pressure application [20]. Compression pressure was found to affect the mass transport in GDL negatively, with increased tortuosity, while simultaneously enhancing electrical conductivity due to reduced bulk and contact resistance [23].

Aside from PTFE coating, electrochemical grafting [24], and direct fluorination methods [25] have been explored to achieve hydrophobicity in GDL. The authors reported some significant improvement in mass transport performance. Facile chemical grafting method was used as a low-cost strategy to fabricate surface-functionalized GDL. The optimized carbon paper showed high porosity, as well as superhydrophobicity property with water contact angle ~150.2° [26]. However, these methods are still plagued with several experimental discrepancies [11].

In PEMFCs, effects of interfacial challenges in GDL are most pronounced at high current densities, leading to concentration polarization and reduced overall power output [27]. These mass transport losses not only reduce energy efficiency below the typical 40-60% for PEMFCs, but also present less value for cost [28,29]. Activation (η_{act}), ohmic (η_{ohm}), and mass transport (η_{conc}) losses account for total performance overpotentials in PEMFCs [29,30]. Below current density of 0.5 A/cm^2, mass transport loss contribution is ~0%. At current densities of 1.0, 1.5, and 2.0 A/cm^2, mass transport loss contribution can be up to 17%, 40%, and 60%, respectively [31]. In *Figure 1(a)*, the percentage deviation (loss) from the theoretical EMF (1.2 V), at each operating range, as indicated in the polarization curve at the mass transport region, is a reflection of how well a theoretical fuel cell is able to remove product water. Below 10% at 1.0 A/cm^2, ~15% at 1.5 A/cm^2, and up to 20% at 2.0 A/cm^2. This is a confirmation that more product water is produced in a fuel cell at current densities >1.0 A/cm^2. Therefore, even though a low PTFE loaded GDL performs efficiently at low current densities, when the cell operates at higher current densities, it experiences flooding. To tackle this, higher PTFE loaded GDLs are employed (*Figure 1(b)*), which leaves the GDL with reduced electronic conductivity.

The effect of water flooding in PEMFCs is reported in *Figure 2*. The electrochemical performance of the cell represented with the polarization curve was not significantly affected when a 10% flooding was experienced in the cell. A significant performance deterioration was seen at 50% flooding. Further significant performance deterioration was reported at 90% flooding, and worse at ~100%.

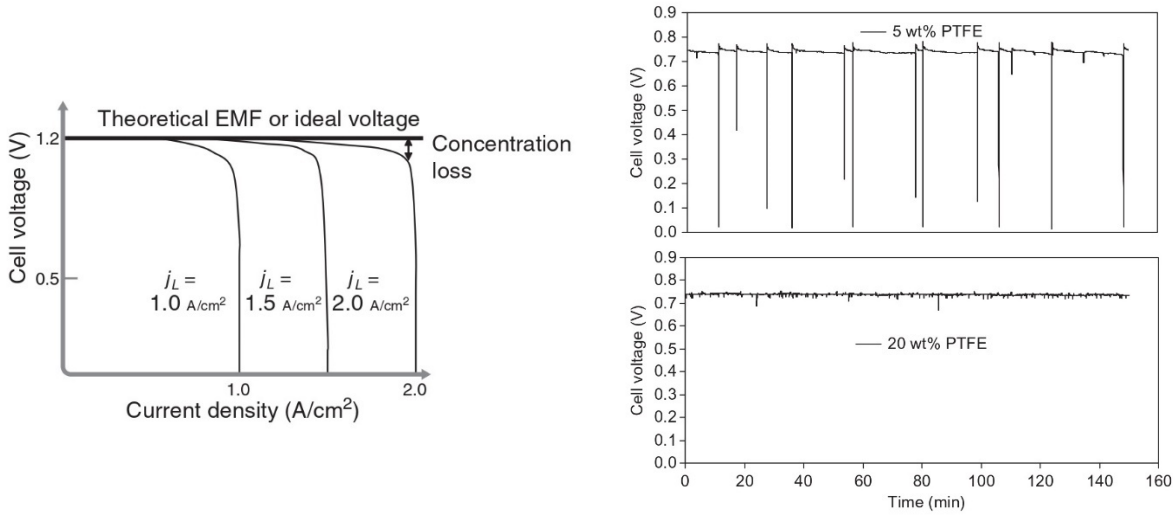


Fig. 1. (a) Theoretical current-voltage plot showing mass transport (concentration) losses on fuel cell performance

Note: The curve clearly indicates significant concentration loss at high current density. Although the concentration loss appears mainly at high current density, its effect is pronounced [29]. (b) Effect of PTFE loading (liquid water flooding) on PEMFC voltage as a function of time at a current density of 0.5 A/cm² [32]

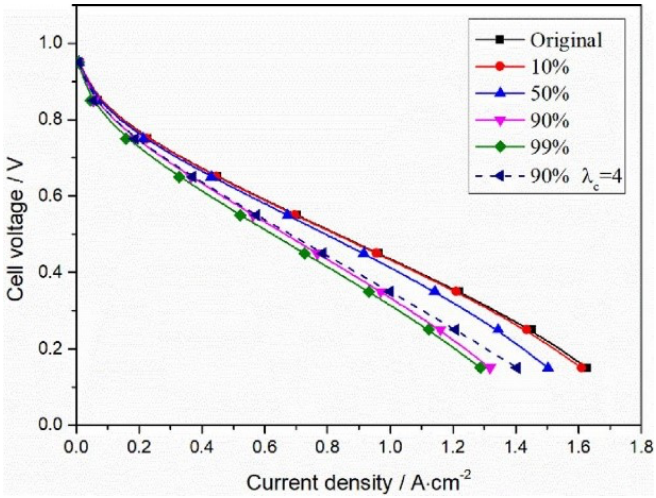


Fig. 2. Effect of different flooding extent on PEMFC performance [33]

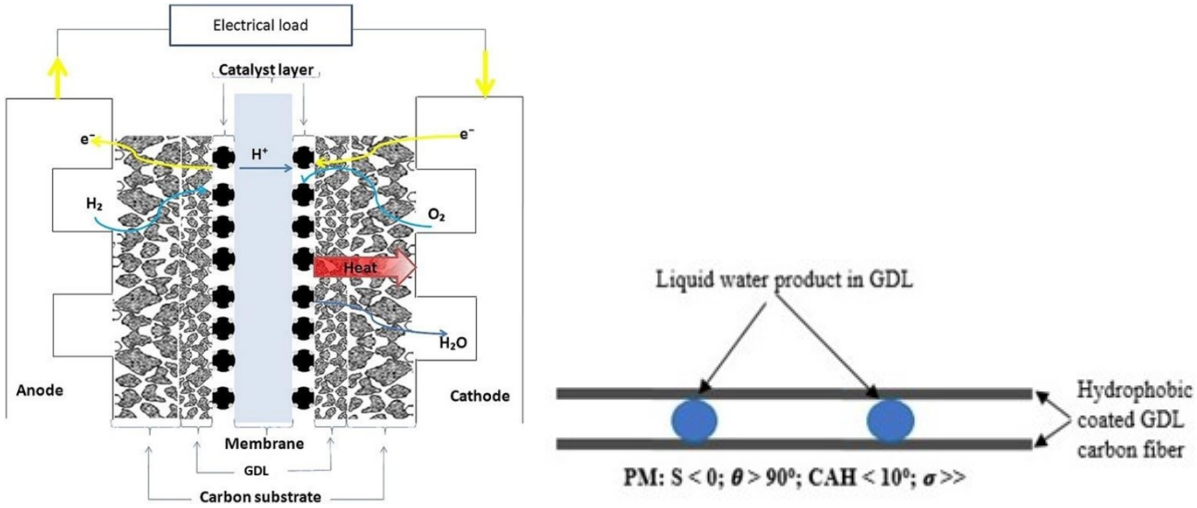
To test the effect of PTFE loading on water flooding, Zhang et al. [32] tested two GDL samples with 5 and 20 wt.% PTFE loadings. From *Figure 1(b)*, it is seen that the 5 wt.% PTFE loading resulted in heavier liquid water flooding than the 20 wt.% PTFE loading. This is because of the hydrophobic property of PTFE, facilitating liquid water removal from the GDL. While this is an effective strategy to address liquid water flooding, at higher current densities (>1.5 A/cm²), more product water is produced at the cathode side. In that case, a further increase in PTFE loading would result in significant reduction in GDL's electronic conductivity.

1.1 Problem Definition

The GDL facilitates the removal of liquid water product on the cathode side of a PEMFC to prevent flooding and the blocking of the catalyst. It is also an electrical conducting medium that transfers

electrons between the catalyst layer and the bipolar plates (*Figure 3(a)*). From the list of interfacial challenges associated with GDL in *Table 1*, this study will be addressing: *(a)* liquid water flooding, *(b)* electrical contact resistance with bipolar plates. Addressing these two GDL interfacial challenges simultaneously would ensure that the desired functionality of the GDL is maintained without the need for trade-offs.

For solving the highlighted challenges, the performance metrics (PM) would include (i) spreading coefficient, S (ii) contact angle, θ (iii) contact angle hysteresis, CAH, for (a), and electronic conductivity, σ, for (b). The interfacial and electronic-conductivity values used throughout this study are referenced against a representative commercial carbon-fiber GDL substrate with typical fiber diameter of ~7-10 μm, areal weight of ~90-120 g/m^2, uncompressed thickness of ~190-280 μm, and bulk porosity of ~70-80%.



(a) (b)

Fig. 3. (a) GDL structure and membrane-electrode-assembly (MEA) sub-components in a PEMFC [7], (b) Schematic of product liquid water permeating through the pores of a hydrophobic coated GDL carbon fiber

Note: Performance metric for this study is stated.

Existing PTFE coatings on GDLs, while highly hydrophobic, reduce through-plane electronic conductivity. This study explores alternative coating materials that can simultaneously sustain hydrophobicity and enhance electronic conductivity – an essential combination for mitigating liquid water flooding and improving PEMFC performance. The subsequent sections of this study detail these analyses.

While electrochemical grafting and direct fluorination have been explored as PTFE alternatives, a low-cost, combustion-derived carbon coating offering wettability comparable to PTFE together with higher intrinsic electronic conductivity has not been systematically evaluated; this is the specific gap addressed here. The objective of this study is to analytically determine whether paraffin candle soot can match or exceed PTFE's spreading coefficient and water contact angle while achieving measurably lower contact-angle hysteresis and higher electronic conductivity than PTFE, using established interfacial and electrochemical models. Improvement over PTFE is therefore assessed against these four measurable criteria.

1.2 Methodology

This study follows an analytical/literature-based research methodology, structured as follows. (a) Research approach: governing interfacial (Girifalco-Good, Young's equation, contact-angle hysteresis) and electrochemical (Butler-Volmer) models are populated with parameters obtained from peer-reviewed literature to analytically evaluate paraffin candle soot against carbon fiber and PTFE. (b) Parameter-selection criteria: literature values are preferentially drawn from studies using carbon-fiber GDL substrates and paraffin-derived or combustion soot, under conditions

closest to typical PEMFC operation (near room temperature, and ambient pressure); where soot-specific data are unavailable, values for chemically analogous carbonaceous materials are used and flagged as such. (c) Uncertainty: literature-derived input parameters carry inherent uncertainty arising from differences in measurement technique, material source, and reporting conditions across studies; this uncertainty propagates into the calculated interfacial energies, spread coefficients, and contact angles reported in Sections 2 and 4. (d) Assumptions: key simplifying assumptions include an interaction parameter $\emptyset = 1$ in the Girifalco-Good equation (justified in Section 2.1), a representative carbon-fiber GDL substrate (Section 1.1), and evaluation at 25 °C as a reference condition (Section 5.3). (e) Limitations: this analytical framework does not include original fabrication, coating deposition, or PEMFC cell testing; all performance projections are theoretical and require experimental validation, as discussed throughout this manuscript.

2. Governing Science and Models

This section presents the interfacial and electrochemical parameters used to evaluate candidate GDL coatings. The spreading coefficient, S, and contact angle, θ, describe equilibrium wettability, whether water beads or spreads on a surface; contact angle hysteresis, CAH, indicates how easily a water droplet detaches and drains from the surface under practical, non-equilibrium conditions; and electronic conductivity, σ, reflects the GDL's ability to transfer electrons between the catalyst layer and bipolar plates. These four metrics were selected because they map directly onto the two interfacial challenges identified in Section 1.1: S, θ, and CAH jointly govern liquid-water flooding behavior, while σ governs electrical contact resistance. Note on units: surface tension and interfacial/surface energy are reported interchangeably in mN/m and mJ/m² in this manuscript and in the cited literature; the two are dimensionally equivalent (both reduce to J/m^2) and are used consistently as such throughout.

2.1 Spreading Analysis

Let the interfacial energies and tensions of solid materials and liquid substances at room temperature (25 °C) be denoted by: GDL carbon fiber in air, γ_{CA} (31.5 mJ/m²) [34], water in air, γ_{WA} (72 mN/m), PTFE in air, γ_{PA} (19 mJ/m²).

We could use the *Girifalco-Good* equation in Eq. 1 [35] to estimate the interfacial energy between two materials (γ_1 & γ_2). An interaction parameter, ϕ , for solid-liquid interfaces is assumed to be 1.

$$\gamma_{12} = \gamma_1 + \gamma_2 - 2\phi\sqrt{\gamma_1\gamma_2} \quad (1)$$

- γ_{CW} = 31.5 + 72 – 2(1)$\sqrt{(31.5)(72)}$ = 8.25 mJ/m²
- γ_{PW} = 19 + 72 – 2(1)$\sqrt{(19)(72)}$ = 17 mJ/m²

The spreading coefficient, S, *of* water *on* carbon fiber *in presence* of air is expressed with Eq. 2 [35]:

$$S_{(W/C)A} = \gamma_{CA} - \gamma_{WA} - \gamma_{CW} \quad (2)$$

- $S_{(W/C)A}$ = 31.5 - 72 - 8.25 = -48.75 (S < 0; partial spreading)

As with Eq. 2, the spreading coefficient, S, *of* water *on* PTFE *in presence* of air is expressed as:

$S_{(W/P)A}$ = 19 - 72 - 17 = *-70* (*S < 0; partial spreading*).

The interaction parameter $\emptyset = 1$ is adopted here as a common simplifying baseline for low-energy, weakly polar carbonaceous and fluoropolymer surfaces in the Girifalco-Good framework, in the absence of soot-specific ∅ data. This is a source of uncertainty, since real soot surfaces are heterogeneous and their composition, graphitic content, and surface functional groups vary with combustion conditions.

2.2 Contact Angle

The equilibrium contact angle, θ_e of water on carbon fiber, and PTFE could be determined using Young's equation in Eq. 3 [35].

$$\cos\theta_e = \frac{\gamma_{SA}-\gamma_{SL}}{\gamma_{LA}} \quad (3)$$

- $\theta_{e(C)}$ = 71° (< 90°, more hydrophilic)
- $\theta_{e(P)}$ = 88° (~ 90°, less hydrophilic)

2.3 Contact Angle Hysteresis

Contact angle hysteresis (CAH) is the difference between the advancing, θ_a, and receding, θ_r contact angles of a liquid substance on a solid surface. It provides information about the surface heterogeneity and how much liquid adheres to the surface [36]. Therefore, for a perfect/slippery surface, CAH ≈ 0°. CAH > 0° for imperfect/sticky surfaces.

For enhanced liquid water management, and easy water mobility in the GDL, CAH is desired to be ~ 0°. That is to say that the surface of the GDL is undesirable to be sticky. This would increase liquid water residence time and eventually cause liquid water flooding. The CAH of water on carbon fiber (CAH_C) [37] and PTFE (CAH_P) [38] are given below:

- $CAH_C = \theta_a - \theta_r$ = 71° (*less slippery*).
- $CAH_P = \theta_a - \theta_r$ = 19.5° (*more slippery*).

2.4 Electronic conductivity

The electrochemical reaction in a PEMFC involves an oxidation reaction at the anode electrode, and a reduction reaction at the cathode electrode. In this system, hydrogen (H_2) oxidizes itself at the anode electrode, and is therefore a reducing agent. Oxygen (O_2) reduces itself at the cathode electrode and is therefore an oxidizing agent.

- Anodic oxidation reaction: $2H_2 \rightarrow 4H^+ + 4e^-$ ($E^o_A = -0V$)
- Cathodic reduction reaction: $O_2 + 4H^+ + 4e^- \rightarrow 2H_2O$ ($E^o_C = +1.23V$)
- Overall galvanic reaction: $2H_2 + O_2 \rightarrow 2H_2O$ ($E^o = +1.23V$)

From the reaction equations above, electrons are released at the anodic reaction site and transferred to the cathodic reaction site. In the GDL, the effective electron conductivity, σ_{eff} is a function of the electron conductivity of the solid carbon fibers and their volume fraction [39].

$$\sigma_{eff} = \sigma_s f(\epsilon) \tag{4}$$

In Eq. 4, σ_{eff} and σ_s are the effective and solid bulk electronic conductivity, respectively, and $f(\epsilon)$ is the structural function based on the porosity, ϵ. This shows that the effective electronic conductivity of the GDL is highly dependent on the bare carbon paper used, and the hydrophobic treatment it undergoes. It is also dependent on the porosity of the carbon fiber, which is a necessary trade-off for reactant and product transport.

Additionally, studies found that the in-plane electron conductivity in GDL is not affected by PTFE loading since electrons would mainly travel through the solid carbon fibers. However, electronic resistivity is increased in the through-plane direction with increased PTFE loading [40]. If σ_C and σ_P are the electronic conductivity of carbon fiber and PTFE loaded GDL, respectively. Then, the ratio, r of the in-plane to the through-plane electronic conductivity of the materials is shown below. Ratio, r = 1 represents highest electronic conductivity, and r > 1 represents loss in electronic conductivity across the through-plane direction. Ratio, r >> 1 represents further loss in electronic conductivity across the through-plane direction due to PTFE loading.

- $r_C = \frac{\sigma_{C(in-plane)}}{\sigma_{C(through-plane)}} = \frac{21{,}000\ S.m^{-1}}{1{,}250\ S.m^{-1}} = 16.8$
- $r_P = \frac{\sigma_{P(in-plane)}}{\sigma_{P(through-plane)}} = \frac{21{,}000\ S.m^{-1}}{850\ S.m^{-1}} = 24.7$
- $\Delta = r_C - r_P = 7.9$ (loss in conductivity due to PTFE loading)

The loss in electronic conductivity of the GDL due to an increase in PTFE loading is seen to deteriorate the performance of the PEMFC. This loss is observed with an increase in the ohmic polarization (η_{ohm}) in *Figure 2*.

Bulk/intrinsic electronic conductivity of a solid material, as used above and in Section 4.1(iv) for paraffin candle soot, is not directly equivalent to the through-plane conductivity realized once that

material is deposited as a coating on a GDL. Coated-GDL through-plane conductivity additionally depends on coating thickness, particle-to-particle and particle-to-fiber contact resistance, coating uniformity, pore blockage, and assembly compression state. Bulk conductivity values reported in this study should therefore be read as an upper-bound indicator rather than a predicted coated-GDL conductivity; direct through-plane resistance measurement of an actual coated sample is required to determine the realized value.

2.5 Electrochemical Reaction Rate

From Faraday's law [29], i = dQ/dt. Thus, current expresses the rate of charge transfer. Each electrochemical reaction event results in the transfer of *n* electrons *(n = 2)*, then:

$$i = nF\frac{dN}{dt} = nFr_x \tag{5}$$

$$r_x = \frac{i}{nF} = \frac{i}{2F} \tag{6}$$

In Eqs. 5 & 6, r_x is the reaction rate, which is dependent on current, i. Furthermore, the electrochemical kinetics of the reaction in a PEM fuel cell is determined using the Butler-Volmer equation [29]:

$$i = i_o \left[\frac{C^s_{red}}{C^{\cdot}_{red}} exp\frac{\alpha_a F}{R_u T}\eta \; - \; \frac{C^s_{ox}}{C^{\cdot}_{ox}} exp\frac{-\alpha_c F}{R_u T}\eta\right] \tag{7}$$

In Eq. 7, current, i, is dependent on the exchange current density, i_o. This is a function of activation voltage loss, η , reaction concentration, C, and charge transfer coefficient, α . R_u is the Universal gas constant, F, Faraday constant, and T, absolute temperature. From Eq. 7, liquid water flooding in the GDL would block the supply of oxygen gas to the cathode reaction site. This causes the reduction of O_2 concentration, increase in η , and reduction in i_o. This results in a slower reaction kinetics.

Physically, liquid water accumulating within GDL pores reduces the effective gas-phase diffusivity available for oxygen transport to the catalyst layer, lowering the local reactant concentration, C, at the cathode reaction site; through Eq. 7 this is expected to reduce exchange current density, i_0, and increase activation overpotential, η. This chain; from reduced flooding to improved oxygen concentration, to faster kinetics, is presented here as a qualitative, mechanistically grounded relationship based on established mass transport and electrochemical kinetics principles, not as a quantitative model calibrated to soot-specific water-removal or transport data. Developing a quantitative droplet-mobility model linking CAH to water-removal rate under realistic operating pressure gradients, and confirming the projected kinetic benefit with polarization curves, exchange-current measurements, and electrochemical impedance spectroscopy, are identified as necessary next steps beyond the present analytical scope.

3. List of Solutions

PTFE functions as a hydrophobic coating on the carbon GDL to enhance its water management property. However, to ensure the GDL retains its electronic conductivity, PTFE content is limited to about 30-35% [6]. Given this loading ratio, periodic flooding remains an issue [8,42] and the GDL could sacrifice thermal and electronic conductivity upon PTFE loading increase [43,44]. *Table 2* presents a list of possible solutions to this challenge.

3.1 Universe of Possible Solutions

Despite significant advances in GDL design for PEMFCs, achieving an optimal balance between hydrophobicity, electronic conductivity, and long-term chemical stability remains a persistent challenge. Conventional PTFE coatings, while effective in imparting hydrophobicity, inherently reduce electronic conductivity when excessively loaded. In recent years, numerous studies have attempted to address this trade-off through various modifications as presented in *Table 3*. However, these approaches are not exhaustive. The present study, therefore, proposes the use of *paraffin candle soot* as an alternative coating for the GDL, aiming to simultaneously improve hydrophobicity, electronic conductivity, and material stability under PEMFC operating conditions.

Table 2. Universe of possible solutions

S/N	Possible solutions	Merit	Demerit	References
1	Increase PTFE loading in GDL	Increases hydrophobicity	Reduces electron conductivity	[43–45]
2	Coating with paraffin candle soot	Increases hydrophobicity & electron conductivity	-	[46]
3	Lotus-leaf impregnation of carbon paper	Increases hydrophobicity	Electron conductivity may be unaffected	[47]
4	Nepenthes pitcher plant impregnation of carbon paper	Enhances liquid water mobility	Does not enhance electron conductivity	[48]
5	Laser ablation/roughening	Increases hydrophobicity	Enhanced contact points may improve electron conductivity	[49]
6	Chemical etching of carbon paper	Removes impurities and improves electron conductivity	Exposes fresh hydrophilic carbon surfaces	[50,51]
7	Polydimethylsiloxane (PDMS) silicone coating	Increased hydrophobicity	Reduces electron conductivity	[52]
8	Silane based coating	Increases hydrophobicity	May slightly reduce electron conductivity	[53]
9	Carbon nanotube (CNT) coating	Increases hydrophobicity & electron conductivity	-	[54,55]

Table 3. Summary of recent studies on GDL hydrophobic coatings and surface modifications

S/N	Coating materials/modifications	Method	Key findings	Remarks	Ref.
1	Carbon paper immersed in methoxy-silanes	Covalent chemical grafting to hydroxylated carbon paper	Carbon paper GDL coated with silanes achieves superhydrophobicity (contact angle ~150°), higher porosity (28.89 µm average pores), and boosts peak power density to 866.4 mW/cm^2. Method is easy to implement and less costly than PTFE/sintering.	The surface modification approach achieved superhydrophobicity. Stability and durability assessments were poorly reported.	[26]
2	Graded electrospun carbon microfibers	Electrospinning with pore-size gradients	The graded GDL improves water management and power output at both low and high RH. Large pore gradients facilitate water removal and reduce ohmic/mass transport resistance, enhancing stability under varying operating conditions.	Comparable electrical conductivity to commercial GDLs, but with less high-frequency resistance (HFR) which is advantageous. Insufficient durability report since microporous layer (MPL) is absent.	[56]
3	PTFE on carbon paper	Waterproofing carbon paper with PTFE	Investigated the addition of PTFE on waterproofed carbon paper. ~6 wt.% and ~13 wt.% PTFE content achieved external and internal waterproofing, respectively. ~37 wt.% PTFE content was found to reduce fuel cell performance.	Increased PTFE content was reported to reduce fuel cell performance.	[57]
4	PTFE on carbon fiber paper	Layered integration of	Combining hydrophilic and hydrophobic pathways in an ultra-thin GDL significantly	Without an MPL, membrane durability, and electronic conductivity	[58]

S/N	Coating materials/modifications	Method	Key findings	Remarks	Ref.
		hydrophilic + hydrophobic carbon membrane	boosts water discharge and management without a MPL. A high limiting current density of 4 A/cm^2 at 0.25 V is achieved, which shows an effective short mass transport pathway.	during extended operation were not reported.	
5	Polyacrylonitrile (PAN)	Insertion into MPL for improved hydrophilicity	3 wt.% PAN addition in the cathode GDL showed 30% higher peak power than hydrophobic GDL under low humidity.	No significant improvement at high humidity (100% RH).	[59]
6	Carbon nanofiber (CNF)	Electro-polymerized polyaniline & carbonization	CNFs were grown in-situ on carbon paper GDL. Results showed a significant increase in pore volume, and superior performance compared to commercial GDL at both high and low humidity conditions.	Achieved better gas and water management. However, durability assessments are yet to be conducted.	[60]
7	PTFE on carbon paper	Scalable mold assembly with a gradient distribution of pore diameters (80-170 μm)	Optimized gradient pore GDL achieved a 20% boost in power density, as well as an optimization of gas-liquid transport.	Particularly addressed gas and liquid transport. Less focus on conductivity, dynamic performance and durability.	[61]
8	PTFE on carbon paper	GDL preparation by spraying, and squeegee coating methods	Results showed that spray coated GDLs had good performance and stability. However, durability was inferior to commercial GDLs.	Carbon corrosion was reported; increase in relative PTFE content; reduced conductivity and performance.	[62]
9	PTFE on carbon paper	Brushing a PTFE solution on carbon paper using triangular, diamond, and inverted triangular patterns	Superior performances were obtained in all cases compared to a uniformly PTFE-treated GDL. Reduced oxygen transport resistance indicative of less water accumulation at the cathode.	Performance results were obtained at 80 ^{o}C. Behavior under supersaturated conditions is yet to be obtained.	[63]
10	Carbon nanotube (CNT)	Developed a fiber-structured MPL with high porosity	Carbon nanofiber shows a higher oriented arrangement of carbon grains after graphitization. High porosity of MPL fiber shows an improved maximum power density (by 47.5%), and maximum current density (by 55.3%) at 100% RH compared to	Achieved significantly improved performances. However, durability assessments are yet to be conducted.	[64]

S/N	Coating materials/modifications	Method	Key findings	Remarks	Ref.
			conventional carbon black particles MPL.		
11	Polydimethylsiloxane (PDMS), and (3-Aminopropyl) triethoxysilane (APTES) on carbon paper	Hydrophobic polymers (PDMS & APTES) were spray coated on carbon GDL surface	Although surfaces containing APTES were found to be more hydrophobic; fuel cells with PDMS recorded superior performance, while those with APTES exhibited better stability at high current densities. PDMS and APTES obtained best performances with (10 wt.%) and (5 wt.%), respectively at 0.6 V.	Comparison was not made with conventional GDLs. Stability and performance issues were reported to be unresolved.	[65]

Novelty relative to other carbon-based coatings: Table 3 shows that silane, carbon-nanofiber, CNT, and conductive-polymer coatings can each achieve favorable wettability or conductivity outcomes, but typically require multi-step synthesis, functionalization, or electro-polymerization processes. Paraffin candle soot's proposed advantage over these alternatives is not superior wettability or conductivity in isolation, but rather its combination of near-zero material cost (a combustion byproduct rather than a synthesized material), single-step deposition simplicity, and an intrinsic conductivity that analytically exceeds PTFE while maintaining comparable wettability (Table 4). Scalability and long-term durability relative to these established alternatives remain to be experimentally established and are not claimed here.

4. Proposed Solution and Rationale for Selection

Wetting occurs when the surface energy of a solid is high enough to overcome the cohesive forces within the water [35]. Paraffin candle soot has low surface energy (γ_{SA} = 22.2 mJ/m^2) [66], typical of carbonaceous materials. This would lead to water droplets forming beads (high contact angles), rather than spreading. The weak interaction between water and paraffin candle soot surface results in a hydrophobic/superhydrophobic and/or even superamphiphobic behavior [46,67].

Coating the carbon fiber of GDL with *paraffin candle soot* is proposed as a rational solution to liquid water flooding in PEMFC. Paraffin is a combination of hydrocarbons derived from petroleum [68], soot produced from paraffin candle is a byproduct of incomplete combustion, composed of carbon particles that form fractal-like nanostructure of interconnected porous carbon (*Figure 4*). These carbon nanostructures have a high electronic conductivity, a large surface area and a mesoporous structure [69]. This soot is found to possess superamphiphobic properties [46,67].

4.1 Rationale for Selection

4.1.1 Spreading Analysis

Let the interfacial energy of paraffin candle soot in air at room temperature (25 ^{o}C) be denoted by γ_{SA} (22.2 mJ/m^2) [66]. From Eq. 1, γ_{SW} is estimated to be 14.24 mJ/m^2.

As with Eq. 2, the spreading coefficient, S, *of* water *on* paraffin candle soot *in presence* of air is expressed as:

- $S_{(W/S)A}$ = 22.2 - 72 - 14.24 = - 64.04 (S < 0; partial spreading).

4.1.2 Contact Angle

The equilibrium contact angle, $\theta_{e(S)}$ of water on paraffin candle soot is determined using Young's equation from Eq. 3.

- $\theta_{e(S)}$ = 83^o (~ 90^o, less hydrophilic).

4.1.3 Contact Angle Hysteresis

The CAH of water on paraffin candle soot (CAH$_S$) [71] is given below:

- $CAH_S = \theta_a - \theta_r = 16^o$ (*more slippery*).

4.1.4 Electronic Conductivity

The electronic conductivity of paraffin candle soot, σ_S can be as high as *127,000 S.m^{-1}* [72]. This is because of their very high surface area.

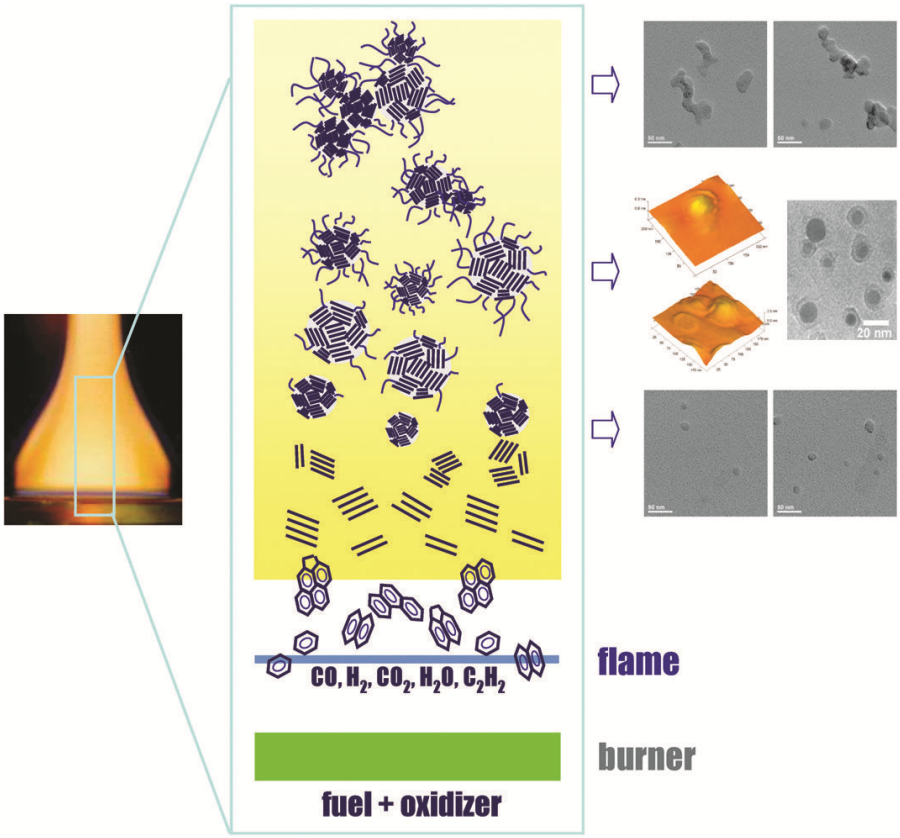


Fig. 4. Schematic illustration of soot deposit and growth in a premixed flat flame [70]

Table 4. Results comparison

S/N	Performance metrics (PM)	Carbon fiber	PTFE	Paraffin candle soot	Remarks
1	Spreading coefficient, S	-48.75	-70	-64.04	S < 0; partial spreading of soot is comparable to PTFE
2	Contact angle, θ	71^o	88^o	83^o	PTFE & soot are ~90^o. They are comparably less hydrophilic.
3	Contact angle hysteresis, CAH	71^o	19.5^o	16^o	Paraffin candle soot is more slippery.
4	Electronic conductivity, σ	21,000/ 1,250 S.m^{-1}	21,000 /850 S.m^{-1}	~127,000 S.m^{-1}	Paraffin candle soot is far more electronically conductive.

5. Overall Systems Enhancement

The analyses in section 4 (*Table 4*) of this study support coating carbon fiber GDL with paraffin candle soot as a promising alternative to PTFE coating. However, further analyses on other interfacial parameters such as adhesion/cohesion, and chemical stability are needed.

5.1 Adhesion/Cohesion of Paraffin Candle Soot

The work of cohesion, *Wc*, of paraffin candle soot refers to the energy required to separate the particles of the material from itself. [46], [73], and [74] reported that paraffin candle soot structure demonstrated fragile cohesive interaction. Chemical vapor deposition technique was suggested as a strategy to improve the cohesive interaction of paraffin candle soot [46], amongst others. The work of cohesion of paraffin candle soot can be determined from its interfacial energy using the relationship in Eq. 8 [35].

$$Wc_{(S)} = 2\gamma_S \tag{8}$$

- $Wc_{(S)} = 2(22.2\ mJ/m^2) = 44.4\ mJ/m^2$ (*weak cohesion*)

On the other hand, the work of adhesion, *Wa*, refers to the energy required to separate paraffin candle soot coating from carbon fiber. The work of adhesion between paraffin candle soot and carbon fiber can be determined from their interfacial energies using the relationship in Eqs. 1 and 9 [35].

$$Wa_{(S\text{-}C)} = \gamma_S + \gamma_C - \gamma_{SC} \tag{9}$$

- $Wa_{(S\text{-}C)} = 22.2\ mJ/m^2 + 31.5\ mJ/m^2 - 0.8\ mJ/m^2 = 52.8\ mJ/m^2$ (*good adhesion*)

Results from the analyses in Eqs. 8 and 9 show that paraffin candle soot coated on carbon fiber GDL will fail by disintegrating within its structure rather than delaminating from the carbon fiber.

Beyond conductive polymeric binders, alternative strategies to improve soot cohesion without the porosity/conductivity penalties associated with excess binder loading include mild thermal post-treatment or partial carbonization of the deposited soot layer (to increase inter-particle graphitic bonding), and controlled, low-loading deposition methods that limit coating thickness while preserving pore connectivity. These alternatives, and the binder-loading trade-off discussed in Section 5.2, remain to be experimentally compared.

5.2 Stability of Paraffin Candle Soot Under PEMFC Operating Conditions

The operating conditions of a fuel cell depend upon the cell, stack, and system design, such that operating parameters like temperature, pressure, flowrate, and humidity become key variables [75]. Low-temperature PEMFCs operate optimally at temperatures between 60 and 90 ^oC [76]. However, high-temperature operating conditions can range from 120 to 200 ^oC [77]. The operating pressure is between 3 and 4 bar [78]. Since paraffin candle soot is a product of incomplete combustion, it has thermal stability up to 300 ^oC [73,74], and can also withstand uniform pressure up to 5 bar [73].

Mechanical compression within the fuel-cell assembly is a further factor not captured by the static stability data above. Compression pressure is known to increase GDL tortuosity while improving electrical contact (Section 1) and is expected to similarly affect a soot coating's pore structure, adhesion under shear, and effective through-plane conductivity; this compression-dependent behavior has not been analytically modeled here and is identified as a required experimental characterization under realistic cell-assembly pressures.

Reactivity tests performed on paraffin candle soot showed that it would remain stable over a wide range of pH values from 1 to 13 [73], and pH values from 2 to 12 [74]. Although it demonstrates high thermal endurance within these ranges, its long-term electrochemical stability under PEMFC operating conditions requires careful consideration. Low-temperature PEMFCs are significantly below the onset temperature for thermal oxidation of carbonaceous materials in air (> 400 ^oC) and far below the conditions required for rapid carbon corrosion [79]. However, oxidation of carbon at the cathode is not purely a thermal process. It is electrochemical and potential-driven. Under transient or start-up/shut-down operating conditions, local electrode potentials (> 0.9 V) can trigger electrochemical oxidation of carbon [80]. This process could lead to gradual loss of the carbon framework and detachment of the coating. Catalytic metal contaminants can also trigger carbon oxidation in PEMFCs, however, this usually occurs at temperatures >100 ^oC [81]. The superiority of paraffin candle soot's electronic conductivity over PTFE which is reported in *Table 4* can be compromised with carbon oxidation, and can also threaten its hydrophobicity [82] during

transient or abnormal operating conditions. On the other hand, PTFE is chemically inert and resistant to oxidative attack [83,84].

The adhesion/cohesion analyses in section 5.1 showed paraffin candle soot to possess better adhesive strength to carbon fiber than the work of cohesion with itself. To improve the cohesive integrity of the paraffin candle soot coating while preserving its favorable electronic and wetting properties, conductive polymeric binders are proposed as suitable candidates. A study by [85] demonstrated that polymers such as polyaniline (PANI), polypyrrole (PPy), and poly(3,4-ethylenedioxythiophene) (PEDOT) can serve as effective conductive binders in carbon-based electrodes because of their conjugated π-electron structures that enable electron delocalization across the coating matrix. These binders improve mechanical adhesion between the carbon fibers and the deposited hydrophobic layer, thus mitigating particle detachment under compression or water shearing during PEMFC operation.

However, the inclusion of polymeric binders can influence porosity, potentially restricting gas permeability and water drainage pathways. At the same time, depending on the polymer's intrinsic conductivity and polarity, electronic conductivity and hydrophobicity may either be maintained or moderately compromised [86,87]. Low binder loadings of conductive polymers in carbon composite electrodes can preserve through-plane conductivity, while excessive loadings can lead to pore blockage and reduced water repellence. Therefore, a balance must be achieved between cohesion and other favorable properties.

Beyond the potential-driven carbon oxidation discussed above, several further PEMFC-relevant durability stressors are not addressed by the present static thermal/chemical stability data and remain to be characterized: repeated humidified hydrogen/oxygen cycling, freeze-thaw cycling below 0 °C, cyclic mechanical compression, and repeated start-up/shut-down transients, which can compound the electrochemical-oxidation risk already noted. Long-term durability testing under these combined, dynamic conditions; rather than static pH, pressure, or temperature exposure alone, is necessary to establish paraffin candle soot's viability relative to PTFE.

5.3 Temperature Dependence of Interfacial Parameters

While PEMFCs typically operate within a temperature range of 60-90 °C, the interfacial data employed in this work were obtained at room temperature (25 °C) because it represents a well-defined reference condition where physical properties such as the surface tension of water, air density, and viscosity are well-established and reproducible. As a result, analytical modeling at room temperature serves as a valid comparative baseline for evaluating trends among materials [88,89].

Table 5. Summary of key physical parameters and data sources

S/N	Parameters	Value	Unit	Sources
1	Interfacial energy of carbon fiber in air, γ_{CA}	31.5	mJ/m^2	[34]
2	Interfacial tension of water in air, γ_{WA}	72	mN/m	[89]
3	Interfacial energy of PTFE in air, γ_{PA}	19	mJ/m^2	[91,92]
4	Electronic conductivity of carbon fiber (in-plane), $\sigma_{C(in-plane)}$	21,000	S.m^{-1}	[41]
5	Electronic conductivity of carbon fiber (through-plane), $\sigma_{C(through-plane)}$	1,250	S.m^{-1}	[41]
6	Electronic conductivity of PTFE (through-plane), $\sigma_{P(through-plane)}$	850	S.m^{-1}	[40]
7	Interfacial energy of paraffin candle soot in air, γ_{SA}	22.2	mJ/m^2	[66]
8	Electronic conductivity of paraffin candle soot, σ_S	127,000	S.m^{-1}	[72]

As temperature increases, molecular kinetic energy rises, leading to a weakening of cohesive forces at the liquid-gas and solid-liquid interfaces. Consequently, both surface and interfacial tensions

decrease approximately linearly with temperature. For liquid water, surface tension decreases from approximately 72 mN/m at 25 °C to about 62 mN/m at 80 °C. [89]. Similar downward trends are observed for interfacial tensions involving air and solid hydrophobic surfaces such as PTFE or carbon-based soot [90]. This reduction implies that as PEMFC operating temperature increases, the liquid-vapor and solid-liquid interfacial energies in Young's equation in Eq. 3 also decrease. The overall balance of interfacial forces at the three-phase contact line is thus altered, leading to a slight reduction in contact angle. Spreading coefficient, S in Eq. 2 also reflects this temperature dependence. S becomes less negative, indicating that the liquid phase experiences a marginally greater tendency to spread over the surface. However, within the typical PEMFC temperature window (60-90 °C), these variations are relatively small, meaning that the overall hydrophobic behavior is preserved. *Table 5* provides a summary of the key physical parameters used in this study.

6. Conclusion

The conclusions below summarize an analytical feasibility assessment based on literature-derived parameters and established interfacial and electrochemical models; they represent analytically predicted, not experimentally demonstrated, outcomes.

The GDL plays a crucial role in ensuring efficient water and gas management in PEMFCs. An ideal GDL material must exhibit high electronic conductivity, controlled porosity, and a balanced degree of hydrophobicity to facilitate reactant diffusion and water removal. Carbon fiber-based substrates have been widely adopted due to their high electronic conductivity and structural integrity; however, their intrinsic hydrophobicity necessitates the use of hydrophobic coatings such as PTFE. Despite PTFE's excellent chemical inertness and thermal stability, excessive loading has been shown to hinder through-plane electronic conductivity.

This study explored the interfacial thermodynamics of paraffin candle soot as an alternative hydrophobic coating to PTFE on carbon fiber GDLs. Based on interfacial energy and spreading coefficient analysis, paraffin candle soot analytically indicated strong potential for maintaining electronic conductivity while providing adequate hydrophobicity, pending experimental confirmation. The material's high adhesion to carbon compared to its weaker cohesion suggests that failure would occur within the soot structure rather than at the soot-substrate interface. To address this cohesive weakness, recent studies suggest a balanced integration of conductive polymer binders into paraffin candle soot-based coatings.

Furthermore, while paraffin candle soot exhibits thermal and chemical stability at normal PEMFC operating conditions; carbon oxidation at the cathode can still occur under high local potentials during start-up/shut-down operations. In contrast, PTFE remains chemically inert under these conditions. Hence, paraffin candle soot-based coatings must be evaluated for electrochemical corrosion resistance and oxidative durability, particularly under transient operation.

In summary, paraffin candle soot presents an attractive, low-cost, and electrically conductive hydrophobic coating for GDLs, offering potential improvements over PTFE. However, its practical viability depends on overcoming key limitations, including: weak cohesion within the soot structure; potential electrochemical oxidation at the cathode under high potentials; limited data on long-term durability under fuel cell humidity and pressure cycling; and temperature-dependent interfacial properties which may marginally affect wettability and performance at elevated operating temperatures.

Nomenclature

C	=	Reaction concentration
CAH	=	Contact angle hysteresis
F	=	Faraday constant
i	=	Current
i_o	=	Exchange current density
R_u	=	Universal gas constant
r_x	=	Reaction rate

S	=	Spreading coefficient
T	=	Temperature
α	=	Charge transfer coefficient
γ	=	Interfacial energy
ε	=	Porosity
η	=	Overpotential/polarization/voltage loss
θ	=	Contact angle
σ	=	Electronic conductivity
φ	=	Interfacial interaction parameter

References

[1] Stoll J, Zhao N, Yuan XZ, et al. Impacts of bubble defects in proton exchange membranes on fuel cell performance and durability. J Power Sources 2024;596. https://doi.org/10.1016/j.jpowsour.2024.234072.

[2] Kumar N, Chen Y, Bahrami M, et al. Quality Implications of Foreign Metallic Particles in the Membrane Electrode Assembly of a Fuel Cell. J Electrochem Soc 2024;171:074513. https://doi.org/10.1149/1945-7111/ad650c.

[3] Liu Q, Lan F, Chen J, et al. A review of proton exchange membrane fuel cell water management: Membrane electrode assembly. J Power Sources 2022;517:230723. https://doi.org/10.1016/j.jpowsour.2021.230723.

[4] Şengül E, Erkan S, Eroğlu İ, et al. Effect Of Gas Diffusion Layer Characteristics And Addition Of Pore-Forming Agents On The Performance Of Polymer Electrolyte Membrane Fuel Cells. Chem Eng Commun 2008;196:161–70. https://doi.org/10.1080/00986440802293130.

[5] Government of Canada. Hydrogen Strategy for Canada: Seizing the Opportunity, A Call to Action. 2020.

[6] Mathur VK, Crawford J. Fundamentals of Gas Diffusion Layers in PEM Fuel Cells. Recent Trends in Fuel Cell Science and Technology, New York, NY: Springer New York; n.d., p. 116–28. https://doi.org/10.1007/978-0-387-68815-2_4.

[7] El-kharouf A, Mason TJ, Brett DJL, et al. Ex-situ characterisation of gas diffusion layers for proton exchange membrane fuel cells. J Power Sources 2012;218:393–404. https://doi.org/10.1016/j.jpowsour.2012.06.099.

[8] Shimpalee S, Beuscher U, Van Zee JW. Analysis of GDL flooding effects on PEMFC performance. Electrochim Acta 2007;52:6748–54. https://doi.org/10.1016/j.electacta.2007.04.115.

[9] Lemoine-Nava R, Hanke-Rauschenbach R, Mangold M, et al. The gas diffusion layer in polymer electrolyte membrane fuel cells: A process model of the two-phase flow. Int J Hydrogen Energy 2011;36:1637–53. https://doi.org/10.1016/j.ijhydene.2010.10.037.

[10] Büchi FN, Boillat P. Polymer Electrolyte Fuel Cells, Mass Transport. Encyclopedia of Applied Electrochemistry, New York, NY: Springer New York; 2014, p. 1661–9. https://doi.org/10.1007/978-1-4419-6996-5_200.

[11] Manzi-Orezzoli V, Mularczyk A, Trtik P, et al. Coating Distribution Analysis on Gas Diffusion Layers for Polymer Electrolyte Fuel Cells by Neutron and X-ray High-Resolution Tomography. ACS Omega 2019;4:17236–43. https://doi.org/10.1021/acsomega.9b01763.

[12] Lian Y, Zheng W, Yue C, et al. Mass transfer capacity degradation of gas diffusion layer under 1000 hours real-world heavy duty load cycles. Int J Heat Mass Transf 2024;223:125239. https://doi.org/10.1016/j.ijheatmasstransfer.2024.125239.

[13] Zhang X, Li S, Huang P, et al. Comparative study on carbon corrosion characteristics of gas diffusion layer in PEMFCs under two accelerated stress tests. Int J Electrochem Sci 2024;19:100581. https://doi.org/10.1016/j.ijoes.2024.100581.

[14] Sim J, Kang M, Min K, et al. Effects of carbon corrosion on proton exchange membrane fuel cell performance using two durability evaluation methods. Renew Energy 2022;190:959–70. https://doi.org/10.1016/j.renene.2022.04.015.

[15] Lædre S, Craciunescu CM, Khoza T, et al. Issues regarding bipolar plate-gas diffusion layer interfacial contact resistance determination. J Power Sources 2022;530:231275. https://doi.org/10.1016/j.jpowsour.2022.231275.

[16] García-Salaberri PA, Vera M, Zaera R. Nonlinear orthotropic model of the inhomogeneous assembly compression of PEM fuel cell gas diffusion layers. Int J Hydrogen Energy 2011;36:11856–70. https://doi.org/10.1016/j.ijhydene.2011.05.152.

[17] Khosravi H S, Abbas Q, Reichmann K. Electrochemical aspects of interconnect materials in PEMFCs. Int J Hydrogen Energy 2021;46:35420–47. https://doi.org/10.1016/j.ijhydene.2021.08.105.

[18] Garzon F, Lopes T, Rockward T, et al. The Impact of Impurities on Long-Term PEMFC Performance. ECS Trans 2009;25:1575–83. https://doi.org/10.1149/1.3210713.

[19] Reshetenko T V. Comprehensive analysis of recovery procedures for SO2-contaminated proton exchange membrane fuel cells. Electrochim Acta 2024;507:145168. https://doi.org/10.1016/j.electacta.2024.145168.
[20] Mathias MF, Roth J, Fleming J, et al. Diffusion media materials and characterisation. Handbook of Fuel Cells, Wiley; 2010. https://doi.org/10.1002/9780470974001.f303046.
[21] Mangal P, Pant LM, Carrigy N, et al. Experimental study of mass transport in PEMFCs: Through plane permeability and molecular diffusivity in GDLs. Electrochim Acta 2015;167:160–71. https://doi.org/10.1016/j.electacta.2015.03.100.
[22] Ito H, Iwamura T, Someya S, et al. Effect of through-plane polytetrafluoroethylene distribution in gas diffusion layers on performance of proton exchange membrane fuel cells. J Power Sources 2016;306:289–99. https://doi.org/10.1016/j.jpowsour.2015.12.020.
[23] Chen J, Gao W, Ning T, et al. Effect of GDL compression on PEMFC performance: A comprehensive cross-scale study. Chemical Engineering Journal 2025;503:158542. https://doi.org/10.1016/j.cej.2024.158542.
[24] Thomas YRJ, Benayad A, Schroder M, et al. New Method for Super Hydrophobic Treatment of Gas Diffusion Layers for Proton Exchange Membrane Fuel Cells Using Electrochemical Reduction of Diazonium Salts. ACS Appl Mater Interfaces 2015;7:15068–77. https://doi.org/10.1021/acsami.5b04428.
[25] Van Nguyen T, Ahosseini A, Wang X, et al. Hydrophobic Gas-Diffusion Media for Polymer-Electrolyte Fuel Cells by Direct Fluorination. J Electrochem Soc 2015;162:F1451–60. https://doi.org/10.1149/2.0411514jes.
[26] Wei X, Zhang Q, Guo J, et al. Surface-Functionalized Gas Diffusion Layer with Chemical-Grafted Superhydrophobic Silanes for Proton Exchange Membrane Fuel Cells. Energy & Fuels 2024;38:6397–402. https://doi.org/10.1021/acs.energyfuels.4c00364.
[27] Winterbone DE, Turan A. Fuel Cells. Advanced Thermodynamics for Engineers, Elsevier; 2015, p. 497–526. https://doi.org/10.1016/B978-0-444-63373-6.00021-6.
[28] U.S. Department of Energy: Energy Efficiency & Renewable Energy. Fuel Cell Technologies Office. 2015.
[29] O'Hayre R, Cha S, Colella W, et al. Fuel Cell Fundamentals. Wiley; 2016. https://doi.org/10.1002/9781119191766.
[30] Mench MM. Fuel Cell Engines. Wiley; 2008. https://doi.org/10.1002/9780470209769.
[31] Barbir F. Main Cell Components, Material Properties, and Processes. PEM Fuel Cells, Elsevier; 2013, p. 73–117. https://doi.org/10.1016/B978-0-12-387710-9.00004-7.
[32] Zhang J, Li H, Shi Z, et al. Effects of Hardware Design and Operation Conditions on PEM Fuel Cell Water Flooding. Int J Green Energy 2010;7:461–74. https://doi.org/10.1080/15435075.2010.515185.
[33] Shen J, Xu L, Chang H, et al. Partial flooding and its effect on the performance of a proton exchange membrane fuel cell. Energy Convers Manag 2020;207:112537. https://doi.org/10.1016/j.enconman.2020.112537.
[34] Wu GM, Schultz JM, Hodge DJ, et al. Effects of treatment on the surface composition and energy of carbon fibers. Polym Compos 1995;16:284–7. https://doi.org/10.1002/pc.750160404.
[35] da Silva LFM, Öchsner A, Adams RD, editors. Handbook of Adhesion Technology. Berlin, Heidelberg: Springer Berlin Heidelberg; 2011. https://doi.org/10.1007/978-3-642-01169-6.
[36] Korhonen JT, Huhtamäki T, Ikkala O, et al. Reliable Measurement of the Receding Contact Angle. Langmuir 2013;29:3858–63. https://doi.org/10.1021/la400009m.
[37] Ko T-J, Her EK, Shin B, et al. Water condensation behavior on the surface of a network of superhydrophobic carbon fibers with high-aspect-ratio nanostructures. Carbon N Y 2012;50:5085–92. https://doi.org/10.1016/j.carbon.2012.06.048.
[38] Kamusewitz H, Possart W. The static contact angle hysteresis obtained by different experiments for the system PTFE/water. Int J Adhes Adhes 1985;5:211–5. https://doi.org/10.1016/0143-7496(85)90013-2.
[39] Zamel N, Li X, Shen J. Numerical estimation of the effective electrical conductivity in carbon paper diffusion media. Appl Energy 2012;93:39–44. https://doi.org/10.1016/j.apenergy.2011.08.037.
[40] Becker J, Flückiger R, Reum M, et al. Determination of Material Properties of Gas Diffusion Layers: Experiments and Simulations Using Phase Contrast Tomographic Microscopy. J Electrochem Soc 2009;156:B1175. https://doi.org/10.1149/1.3176876.
[41] Fuel Cell Earth. Toray Carbon Fiber Paper 'TGP-H''.' n.d.
[42] Chen H, Zhang R, Xia Z, et al. Experimental investigation on PEM fuel cell flooding mitigation under heavy loading condition. Appl Energy 2023;349:121632. https://doi.org/10.1016/j.apenergy.2023.121632.
[43] Sadeghifar H, Djilali N, Bahrami M. Effect of Polytetrafluoroethylene (PTFE) and micro porous layer (MPL) on thermal conductivity of fuel cell gas diffusion layers: Modeling and experiments. J Power Sources 2014;248:632–41. https://doi.org/10.1016/j.jpowsour.2013.09.136.

[44] Ismail MS, Damjanovic T, Ingham DB, et al. Effect of polytetrafluoroethylene-treatment and microporous layer-coating on the electrical conductivity of gas diffusion layers used in proton exchange membrane fuel cells. J Power Sources 2010;195:2700–8. https://doi.org/10.1016/j.jpowsour.2009.11.069.
[45] Chen T, Liu S, Zhang J, et al. Study on the characteristics of GDL with different PTFE content and its effect on the performance of PEMFC. Int J Heat Mass Transf 2019;128:1168–74. https://doi.org/10.1016/j.ijheatmasstransfer.2018.09.097.
[46] Deng X, Mammen L, Butt H-J, et al. Candle Soot as a Template for a Transparent Robust Superamphiphobic Coating. Science (1979) 2012;335:67–70. https://doi.org/10.1126/science.1207115.
[47] Li G, Jiang B, Liu H, et al. Superhydrophobic surface with lotus/petal effect and its improvement on fatigue resistance of heat-resistant steel. Prog Org Coat 2019;137:105315. https://doi.org/10.1016/j.porgcoat.2019.105315.
[48] Wong T-S, Kang SH, Tang SKY, et al. Bioinspired self-repairing slippery surfaces with pressure-stable omniphobicity. Nature 2011;477:443–7. https://doi.org/10.1038/nature10447.
[49] Du Q, Zhou P, Pan Y, et al. Influence of hydrophobicity and roughness on the wetting and flow resistance of water droplets on solid surface: A many-body dissipative particle dynamics study. Chem Eng Sci 2022;249:117327. https://doi.org/10.1016/j.ces.2021.117327.
[50] Taskin NU, Ordu F. Effect of etching duration on roughness and wettability of different carbon steel substrates. Mater Chem Phys 2021;257:123746. https://doi.org/10.1016/j.matchemphys.2020.123746.
[51] Qian B, Shen Z. Fabrication of Superhydrophobic Surfaces by Dislocation-Selective Chemical Etching on Aluminum, Copper, and Zinc Substrates. Langmuir 2005;21:9007–9. https://doi.org/10.1021/la051308c.
[52] Lipika, Singh AK. Polydimethylsiloxane based sustainable hydrophobic/oleophilic coatings for oil/water separation: A review. Cleaner Materials 2022;6:100136. https://doi.org/10.1016/j.clema.2022.100136.
[53] Nie Y, Ma S, Tian M, et al. Superhydrophobic silane-based surface coatings on metal surface with nanoparticles hybridization to enhance anticorrosion efficiency, wearing resistance and antimicrobial ability. Surf Coat Technol 2021;410:126966. https://doi.org/10.1016/j.surfcoat.2021.126966.
[54] Oh M, Seo H, Choi J, et al. Transition of Carbon Nanotube Sheets from Hydrophobicity to Hydrophilicity by Facile Electrochemical Wetting. Nanomaterials 2023;13:2834. https://doi.org/10.3390/nano13212834.
[55] Okafor O, Popoola A, Popoola O, et al. Surface modification of carbon nanotubes and their nanocomposites for fuel cell applications: A review. AIMS Mater Sci 2024;11:369–414. https://doi.org/10.3934/matersci.2024020.
[56] Balakrishnan M, Shrestha P, Ge N, et al. Designing Tailored Gas Diffusion Layers with Pore Size Gradients via Electrospinning for Polymer Electrolyte Membrane Fuel Cells. ACS Appl Energy Mater 2020;3:2695–707. https://doi.org/10.1021/acsaem.9b02371.
[57] Yoshimune W, Kato A, Yamaguchi S, et al. Comprehensive Analysis of Wettability in Waterproofed Gas Diffusion Layers for Polymer Electrolyte Fuel Cells. ACS Appl Mater Interfaces 2024;16:36489–97. https://doi.org/10.1021/acsami.4c07867.
[58] Liu H, Zhang J, Wang B. Ultra-thin gas diffusion layer with integrated hydrophobic and hydrophilic paths for enhanced water management performance of proton exchange membrane fuel cells. Int J Hydrogen Energy 2025;144:1–7. https://doi.org/10.1016/j.ijhydene.2025.06.011.
[59] Liu Z, Zhou L, Gao Y, et al. A novel hydrophilic-modified gas diffusion layer for proton exchange membrane fuel cells operating in low humidification. Int J Energy Res 2021;45:16874–83. https://doi.org/10.1002/er.6844.
[60] Liu C, Li S. Performance Enhancement of Proton Exchange Membrane Fuel Cell through Carbon Nanofibers Grown In Situ on Carbon Paper. Molecules 2023;28:2810. https://doi.org/10.3390/molecules28062810.
[61] Wang R-X, Chen B-H, Wang Y-F-H, et al. Enhancing Fuel Cell Performance by Constructing a Gas Diffusion Layer with Gradient Microstructure. Materials 2025;18:3271. https://doi.org/10.3390/ma18143271.
[62] Li T, Zhou K, Lin G. Study on preparation process and durability of gas diffusion layer of proton exchange membrane fuel cell. Ionics (Kiel) 2022;28:1387–401. https://doi.org/10.1007/s11581-022-04439-0.
[63] Calili-Cankir F, Can EM, Ingham DB, et al. Patterned hydrophobic gas diffusion layers for enhanced water management in polymer electrolyte fuel cells. Chemical Engineering Journal 2024;484:149711. https://doi.org/10.1016/j.cej.2024.149711.
[64] Yu M, Cui H, Tao J, et al. Fabrication of novel carbon nanofiber membrane microporous layer to improve water management ability of PEMFC. Journal of Industrial Textiles 2025;55. https://doi.org/10.1177/15280837251315070.
[65] UNGAN H, BAYRAKÇEKEN YURTCAN A. Water management improvement in PEM fuel cells via addition of PDMS or APTES polymers to the catalyst layer. Turk J Chem 2020;44:1227–43. https://doi.org/10.3906/kim-2002-49.

[66] Jańczuk B, Białopiotrowicz T. The total surface free energy and the contact angle in the case of low energetic solids. J Colloid Interface Sci 1990;140:362–72. https://doi.org/10.1016/0021-9797(90)90356-S.
[67] Mansor M, Budiman SN, Paad KM, et al. Physicochemical Characterization of Candle Soot Functionalized with Nitric Acid. Chem Eng Trans 2023;106:1135–40. https://doi.org/10.3303/CET23106190.
[68] Kumar V, Pallapa M, Rezai P, et al. Polymers. Reference Module in Materials Science and Materials Engineering, Elsevier; 2016. https://doi.org/10.1016/B978-0-12-803581-8.00522-1.
[69] Mulay MR, Chauhan A, Patel S, et al. Candle soot: Journey from a pollutant to a functional material. Carbon N Y 2019;144:684–712. https://doi.org/10.1016/j.carbon.2018.12.083.
[70] Cain JP, Gassman PL, Wang H, et al. Micro-FTIR study of soot chemical composition—evidence of aliphatic hydrocarbons on nascent soot surfaces. Physical Chemistry Chemical Physics 2010;12:5206. https://doi.org/10.1039/b924344e.
[71] Bär RM, Widmaier S, Levkin PA. Facile fabrication of robust superhydrophobic surfaces: comparative investigation. RSC Adv 2016;6:98257–66. https://doi.org/10.1039/C6RA22336B.
[72] Vishwanath HS, Rao AHN, Mundinamani S, et al. Highly conductive candle-soot-based polymer composite as a conductive ink for electronic applications. Journal of Materials Science: Materials in Electronics 2024;35:2008. https://doi.org/10.1007/s10854-024-13763-2.
[73] Seo K, Kim M, Kim DH. Candle-based process for creating a stable superhydrophobic surface. Carbon N Y 2014;68:583–96. https://doi.org/10.1016/j.carbon.2013.11.038.
[74] Xiao L, Zeng W, Liao G, et al. Thermally and Chemically Stable Candle Soot Superhydrophobic Surface with Excellent Self-Cleaning Properties in Air and Oil. ACS Appl Nano Mater 2018;1:1204–11. https://doi.org/10.1021/acsanm.7b00363.
[75] Jang J-H, Chiu H-C, Yan W-M, et al. Effects of operating conditions on the performances of individual cell and stack of PEM fuel cell. J Power Sources 2008;180:476–83. https://doi.org/10.1016/j.jpowsour.2008.02.001.
[76] Tang X, Zhang Y, Xu S. Temperature sensitivity characteristics of PEM fuel cell and output performance improvement based on optimal active temperature control. Int J Heat Mass Transf 2023;206:123966. https://doi.org/10.1016/j.ijheatmasstransfer.2023.123966.
[77] Rosli RE, Sulong AB, Daud WRW, et al. A review of high-temperature proton exchange membrane fuel cell (HT-PEMFC) system. Int J Hydrogen Energy 2017;42:9293–314. https://doi.org/10.1016/j.ijhydene.2016.06.211.
[78] Ahmadi N, Dadvand A, Rezazadeh S, et al. Analysis of the operating pressure and GDL geometrical configuration effect on PEM fuel cell performance. Journal of the Brazilian Society of Mechanical Sciences and Engineering 2016;38:2311–25. https://doi.org/10.1007/s40430-016-0548-0.
[79] Sádovská G, Honcová P, Morávková J, et al. The thermal stability of carbon materials in the air: Quantitative structural investigation of thermal stability of carbon materials in air. Carbon N Y 2023;206:211–25. https://doi.org/10.1016/j.carbon.2023.02.042.
[80] Zhao J, Tu Z, Chan SH. Carbon corrosion mechanism and mitigation strategies in a proton exchange membrane fuel cell (PEMFC): A review. J Power Sources 2021;488:229434. https://doi.org/10.1016/j.jpowsour.2020.229434.
[81] Komini Babu S, Spernjak D, Dillet J, et al. Spatially resolved degradation during startup and shutdown in polymer electrolyte membrane fuel cell operation. Appl Energy 2019;254:113659. https://doi.org/10.1016/j.apenergy.2019.113659.
[82] Zuberi B, Johnson KS, Aleks GK, et al. Hydrophilic properties of aged soot. Geophys Res Lett 2005;32. https://doi.org/10.1029/2004GL021496.
[83] Sanders IC, Oberlander KA, Spearrin RM. Polytetrafluoroethylene (PTFE) burn characteristics and toxicant formation in an oxidizer cross-flow via laser absorption tomography. Proceedings of the Combustion Institute 2024;40:105394. https://doi.org/10.1016/j.proci.2024.105394.
[84] Yu H, Idesaki A, Yoshimura K, et al. Effects of temperature on the decomposition of PTFE induced by electron beam irradiation. Radiation Physics and Chemistry 2025;237:113029. https://doi.org/10.1016/j.radphyschem.2025.113029.
[85] Yazdani McCord MR, Seppälä A, Pourakbari-Kasmaei M, et al. From low conductivity to high energy efficiency: The role of conductive polymers in phase change materials. Chemical Engineering Journal 2025;508:160804. https://doi.org/10.1016/j.cej.2025.160804.
[86] Zhang W, Dehghani-Sanij AA, Blackburn RS. Carbon based conductive polymer composites. J Mater Sci 2007;42:3408–18. https://doi.org/10.1007/s10853-007-1688-5.
[87] Del Olmo R, Guzmán-González G, Sanz O, et al. Versatile mixed ionic-electronic conducting binders for high-power, high-energy batteries. Electrochim Acta 2024;474:143547. https://doi.org/10.1016/j.electacta.2023.143547.

[88] Guo J, Wang R, Zhang S, et al. Temperature Dependency of the Apolar Surface Tension Component for Water and Its Role in Classifying Apolar and Polar Interfacial Interactions. The Journal of Physical Chemistry C 2023;127:18167–75. https://doi.org/10.1021/acs.jpcc.3c04095.
[89] Vargaftik NB, Volkov BN, Voljak LD. International Tables of the Surface Tension of Water. J Phys Chem Ref Data 1983;12:817–20. https://doi.org/10.1063/1.555688.
[90] Hamieh T. The Effect of the Temperature on the Surface Energetic Properties of Carbon Fibers by Inverse Gas Chromatography 2023. https://doi.org/10.20944/preprints202311.1908.v1.
[91] Bascom WD. The wettability of polymer surfaces and the spreading of polymer liquids, 1988, p. 89–124. https://doi.org/10.1007/BFb0024051.
[92] Durkee J. Testing for cleanliness. Management of Industrial Cleaning Technology and Processes, Elsevier; 2006, p. 257–93. https://doi.org/10.1016/B978-008044888-6/50019-3.